

Fig. SM1. A plot of particle size distribution of CFBC fly ash

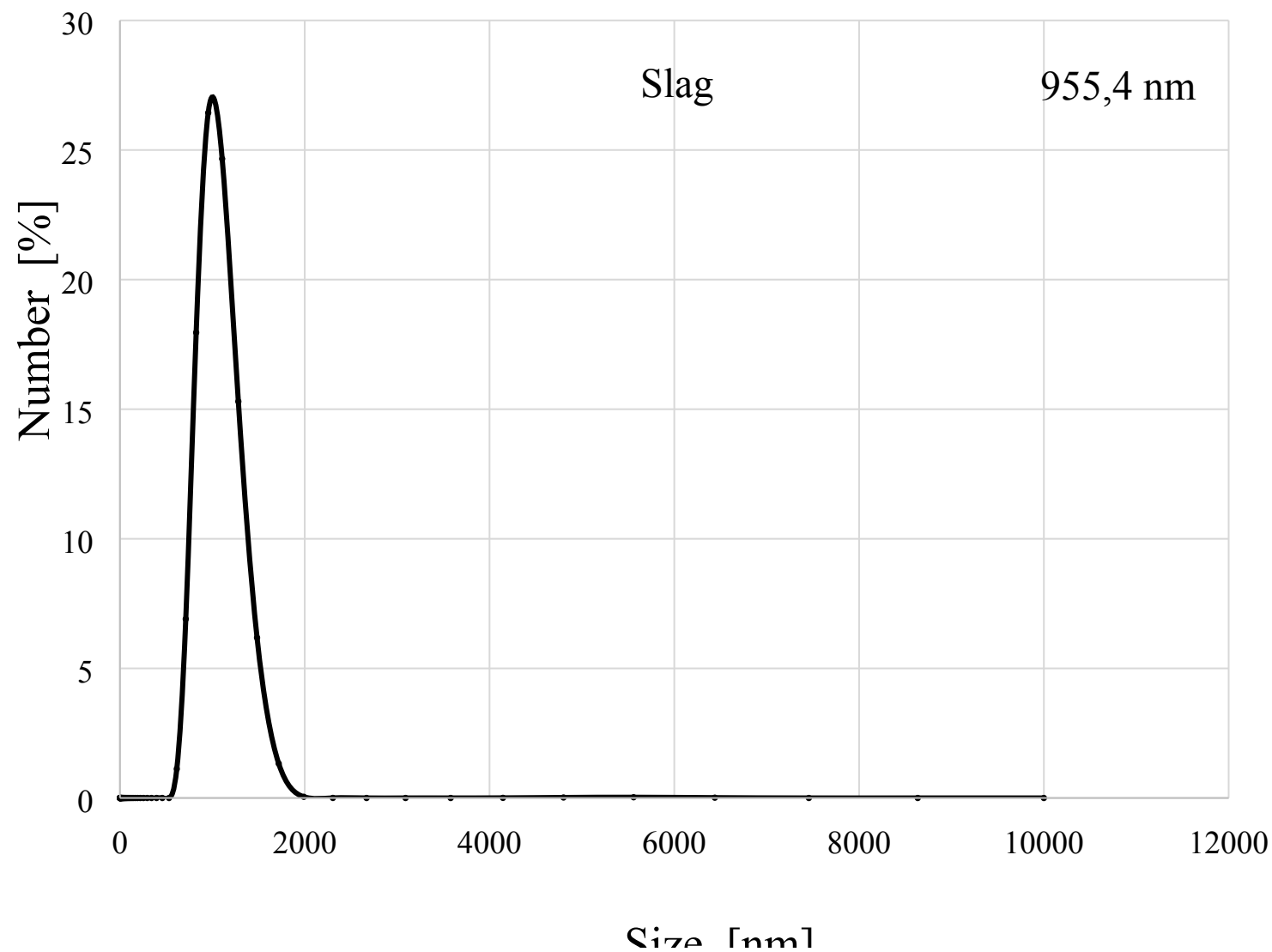


Fig. SM2. A plot of particle size distribution of CFBC slag

Full scale counts: 12785

Base(18)_pt1

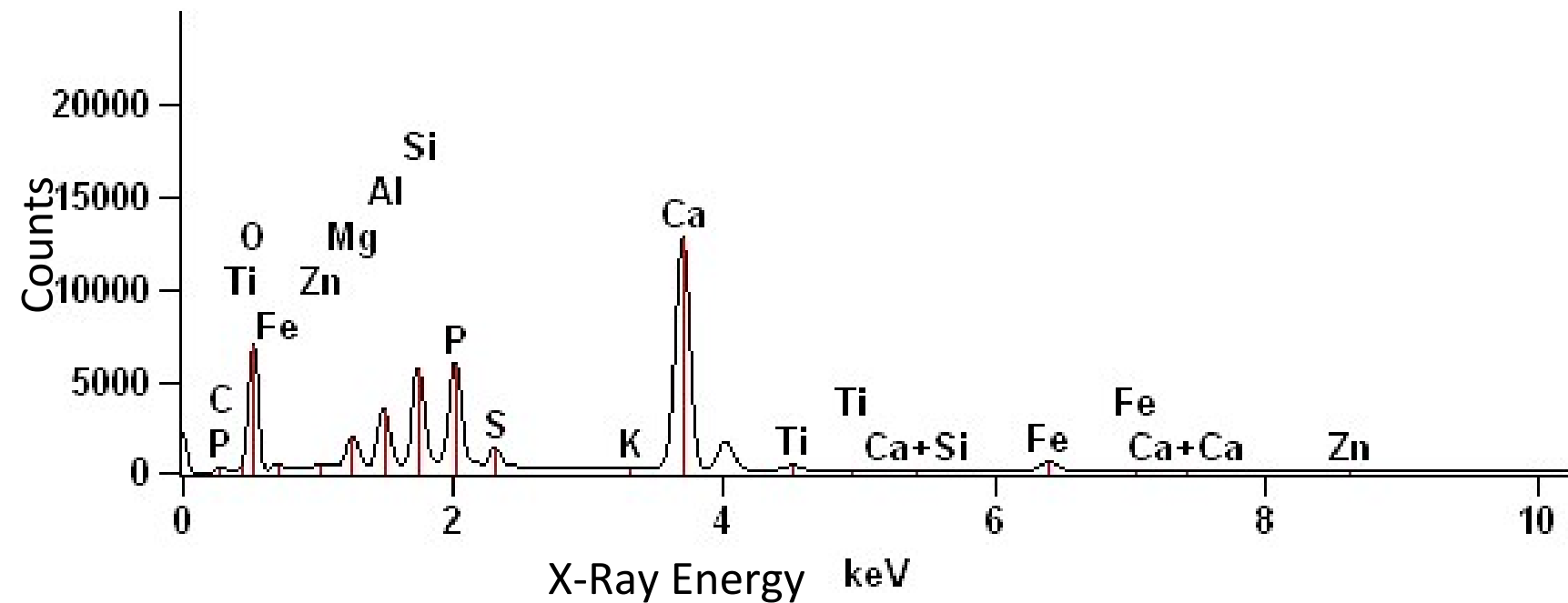


Fig. SM3. EDS spectrum of CFBC fly ash (magn. x200)

Full scale counts: 14929

Base(16)_pt2

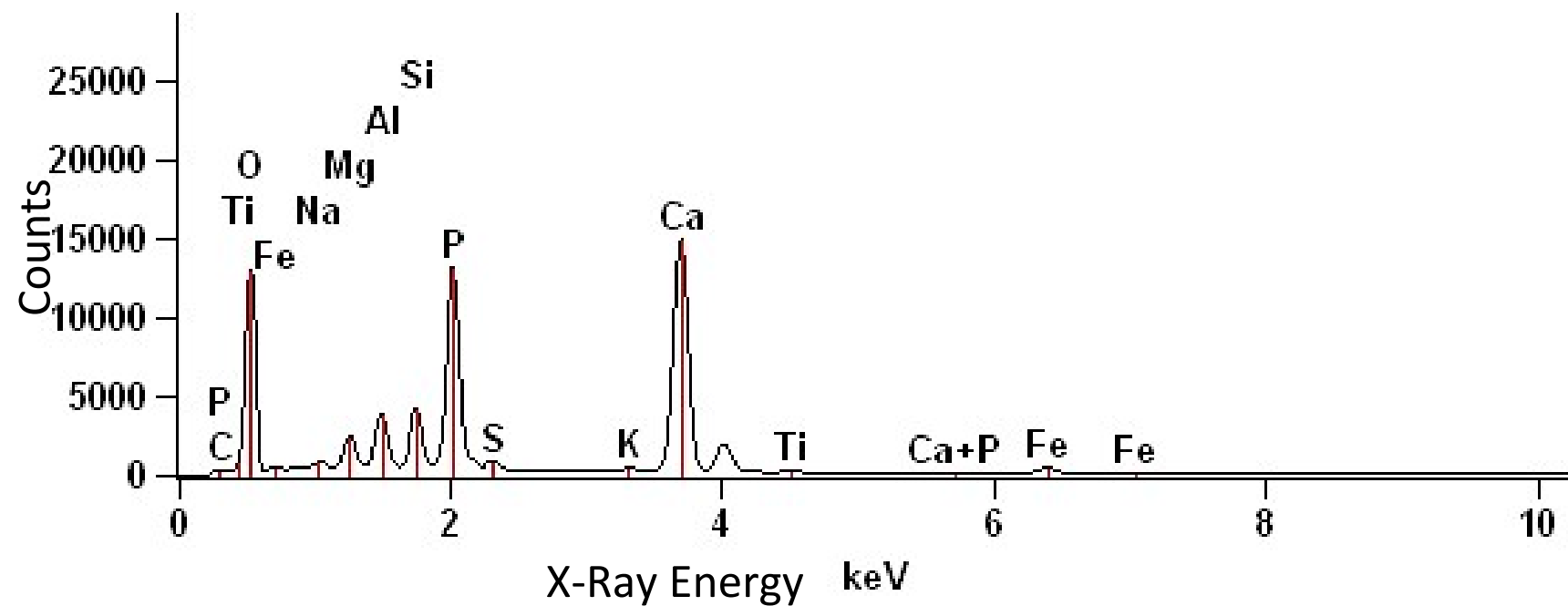


Fig. SM4. EDS spectrum of CFBC slag (magn. x200)

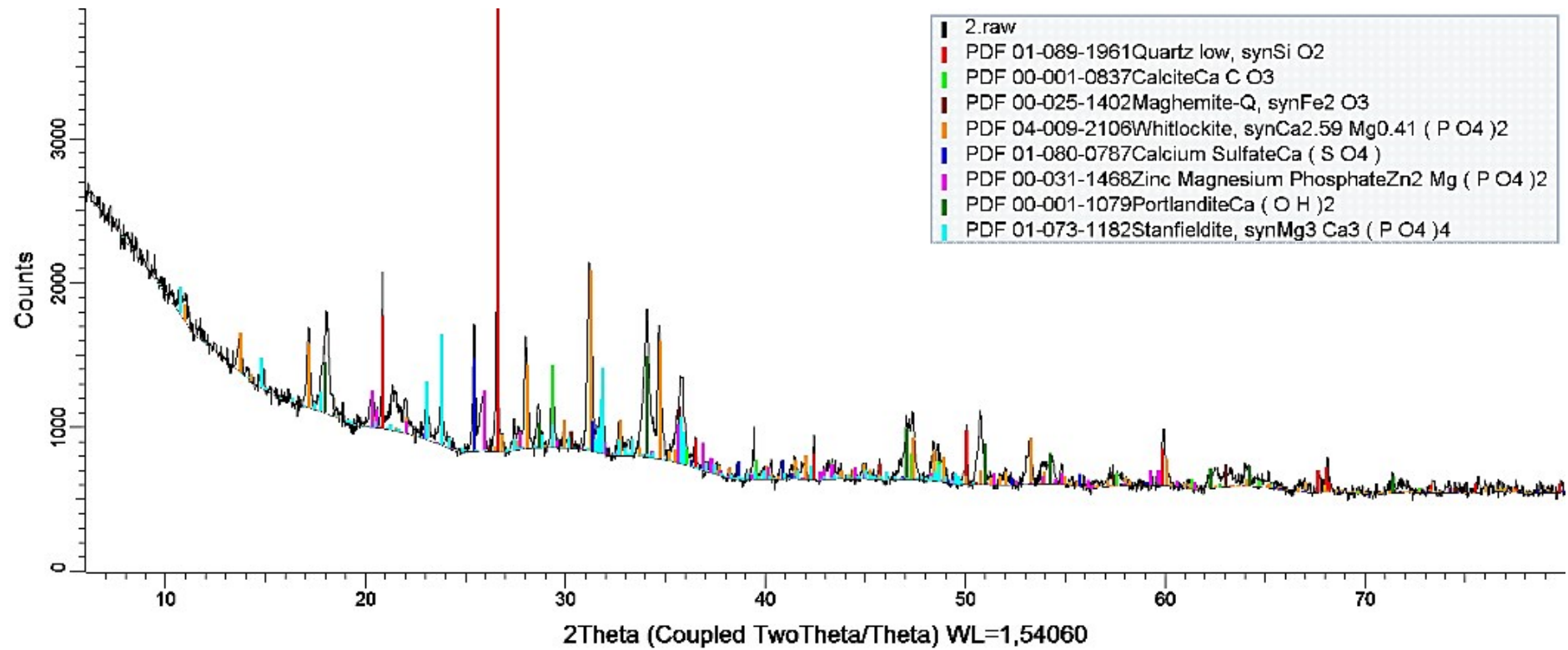


Fig. SM5. X-ray diffraction pattern of CFBC fly ash

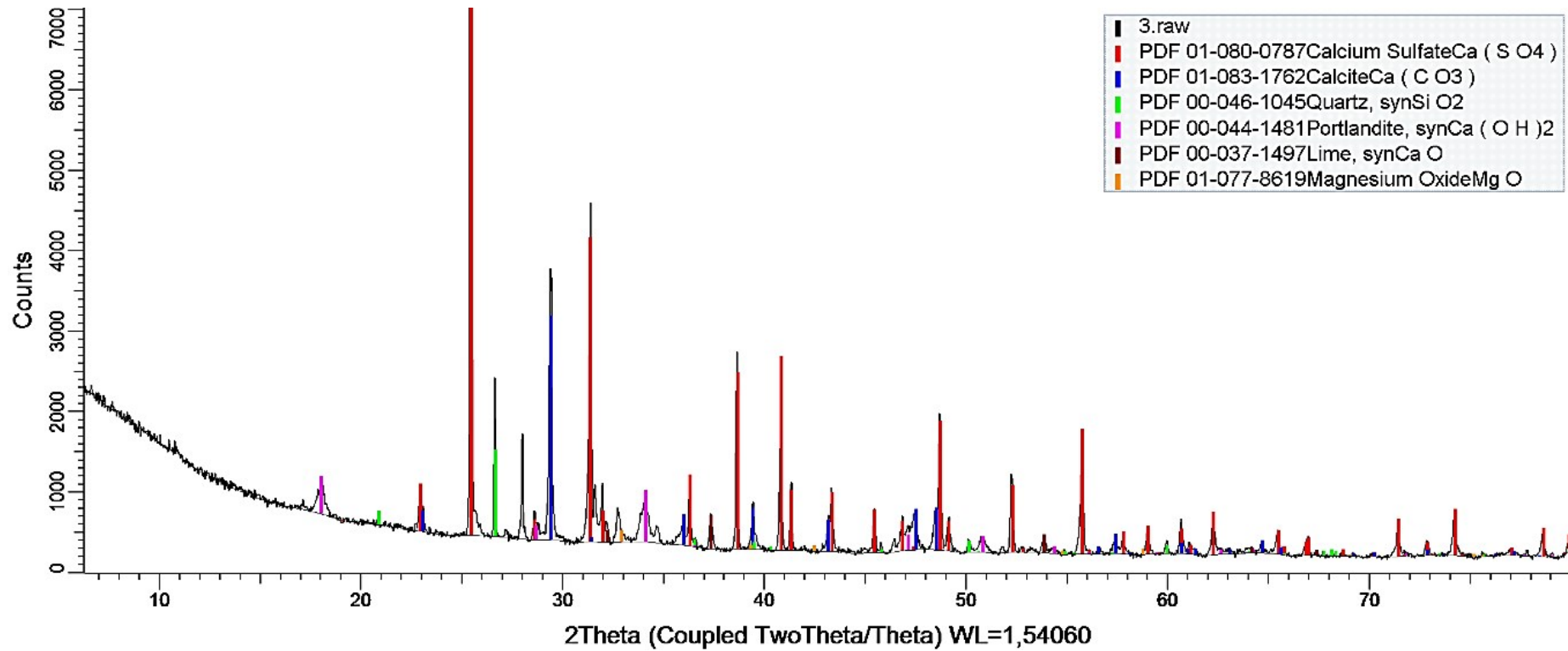


Fig. SM6. X-ray diffraction pattern of CFBC slag

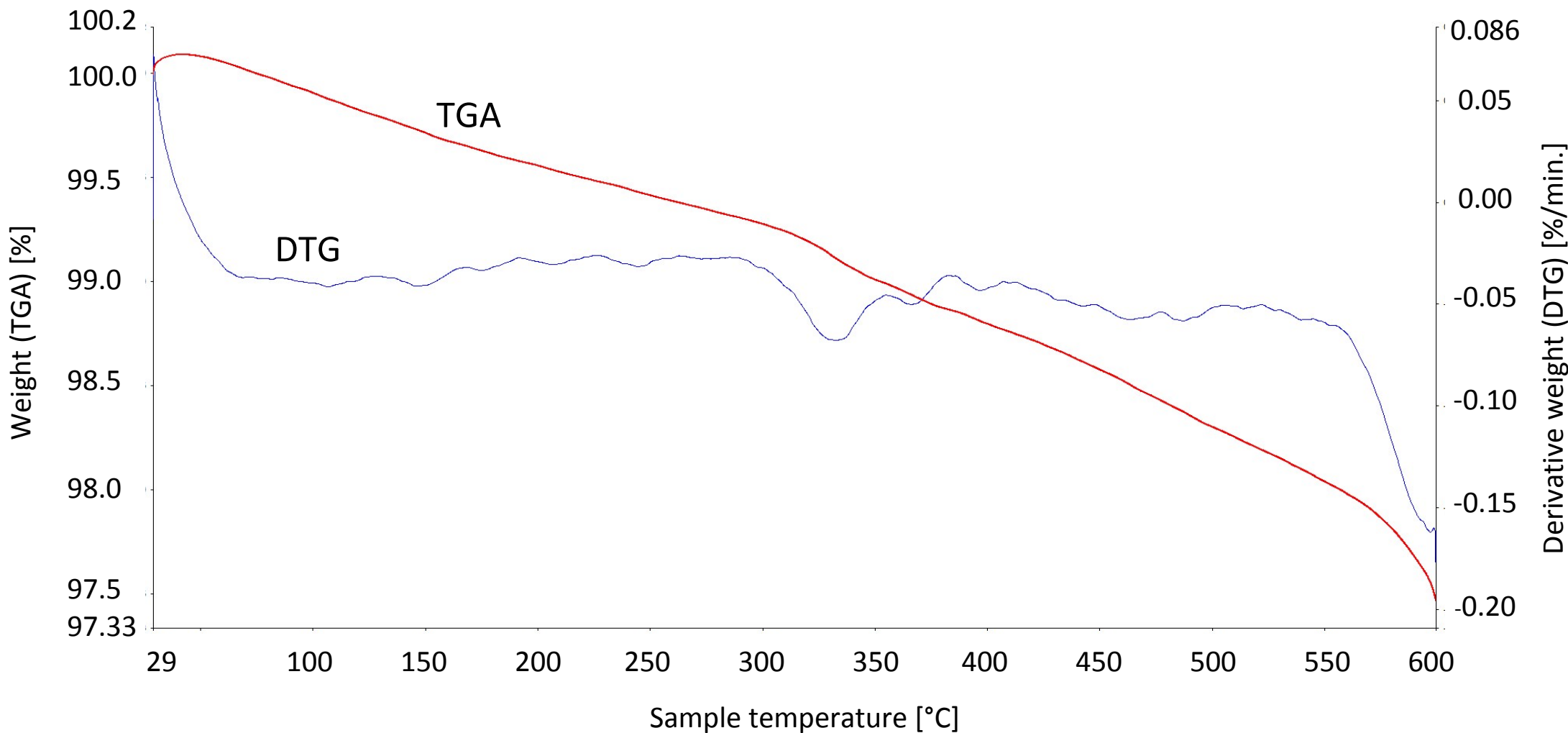


Fig. SM7. Thermogravimetric curves of CFBC fly ash

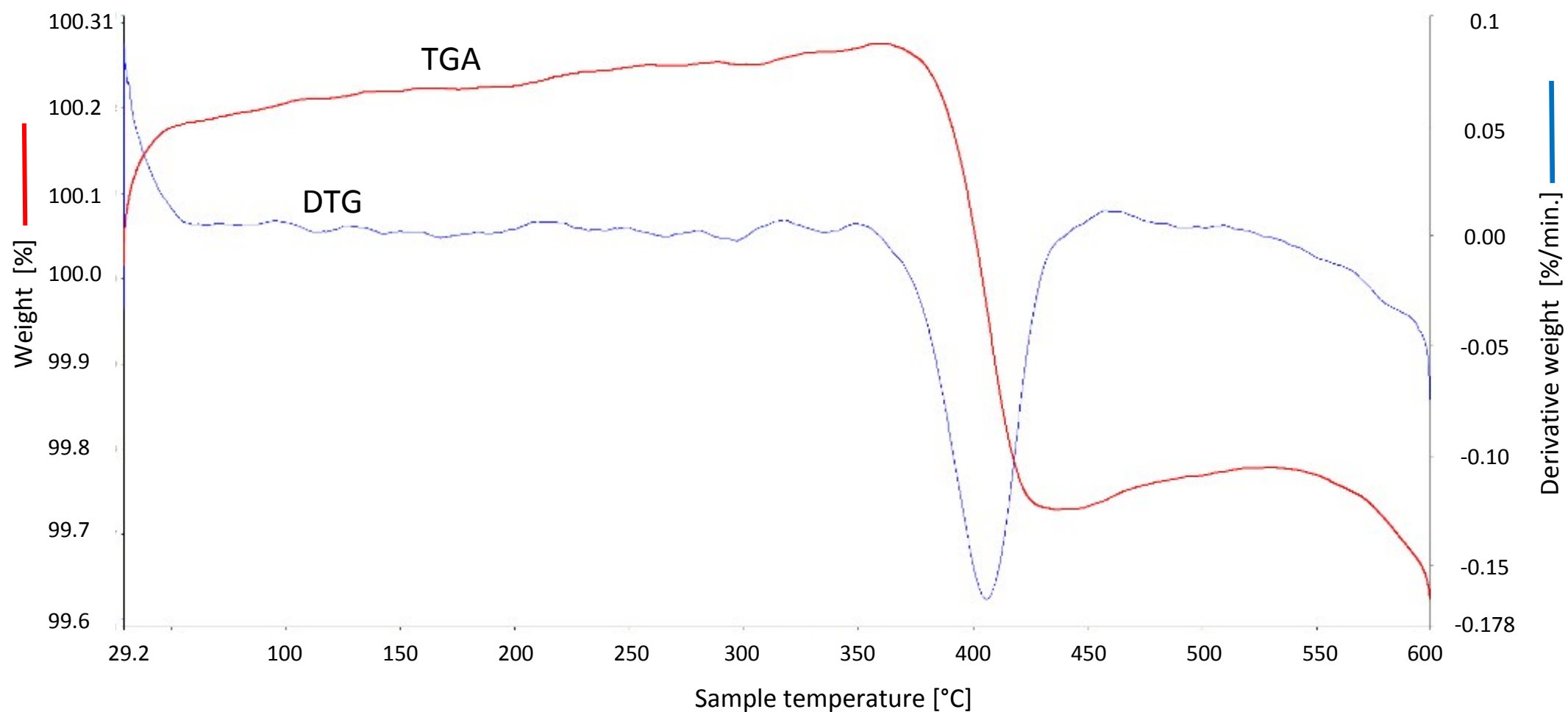


Fig. SM8. Thermogravimetric curves of CFBC slag

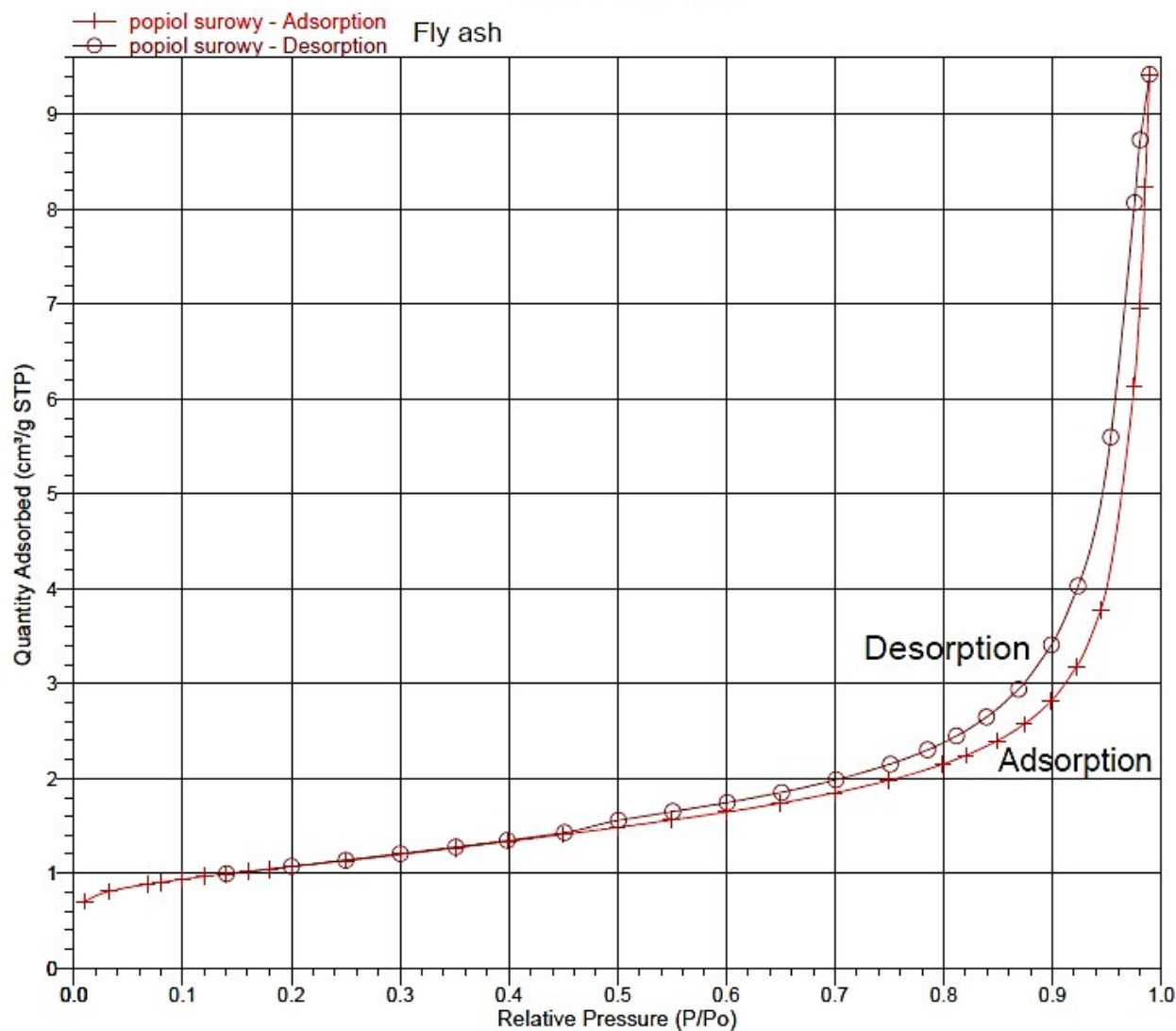


Fig. SM9. The low temperature BET adsorption and desorption isotherms of CFBC fly ash

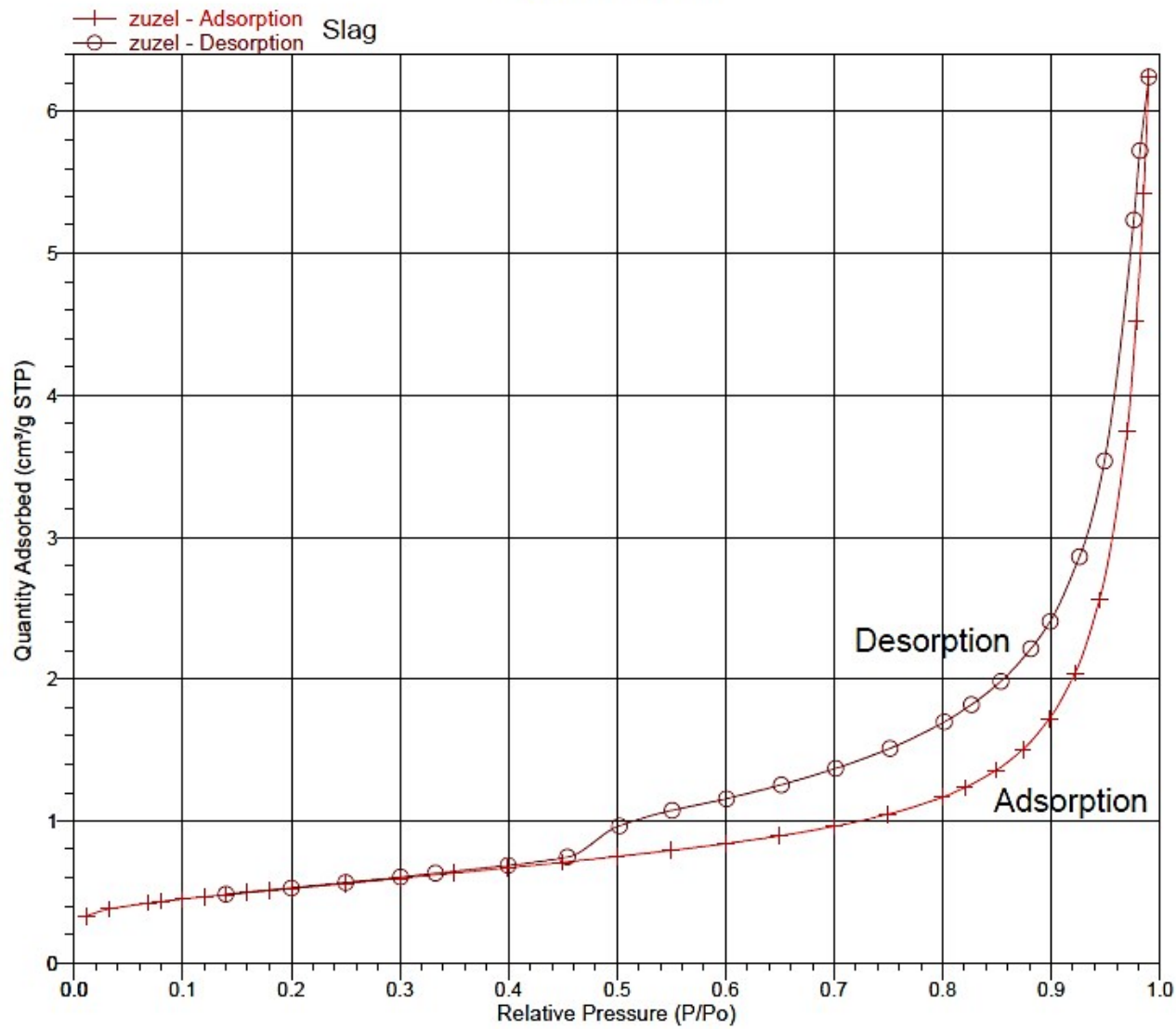


Fig. SM10. The low temperature BET adsorption and desorption isotherms of CFBC slag

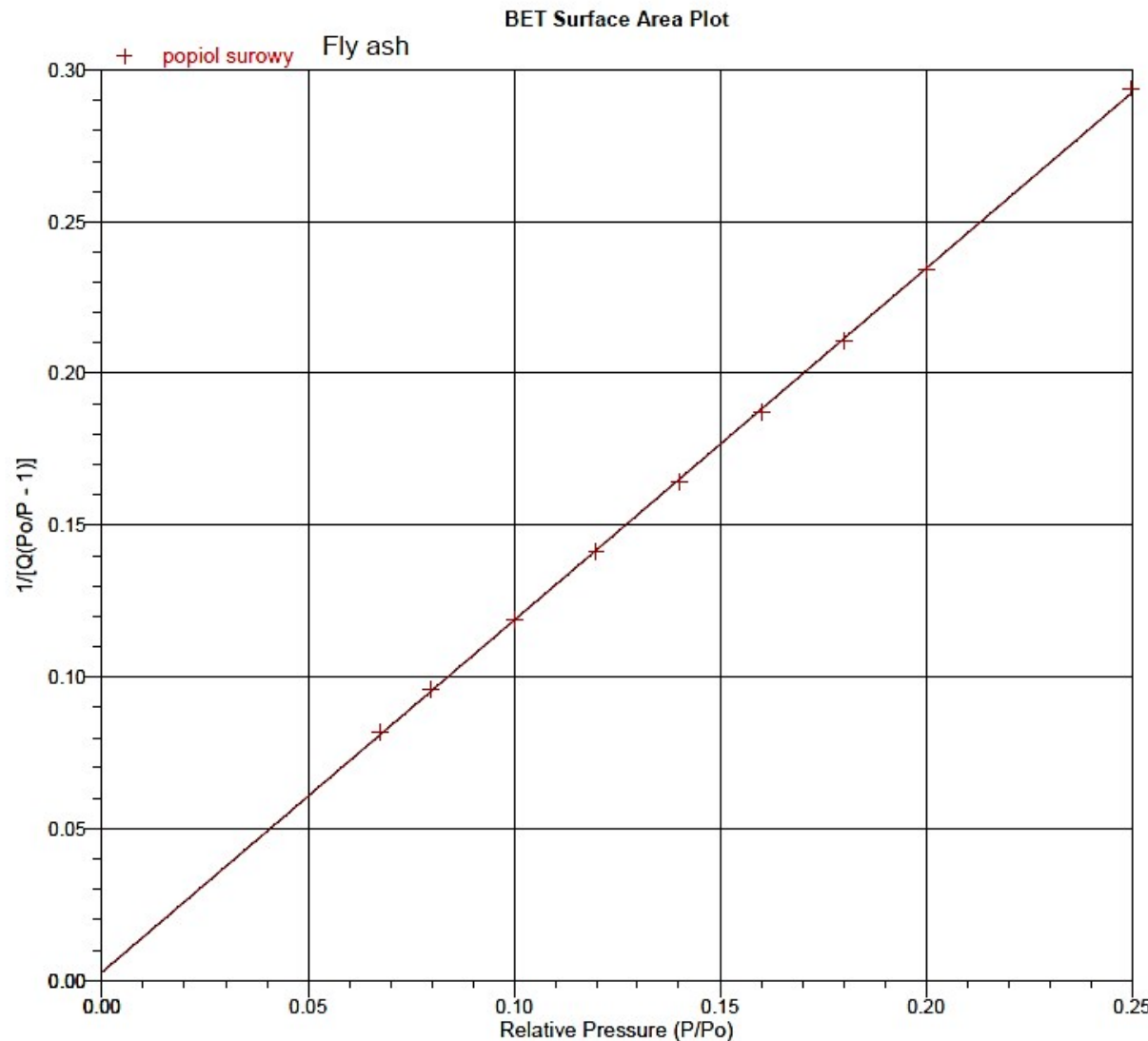


Fig. SM11. The linear BET isotherm of CFBC fly ash

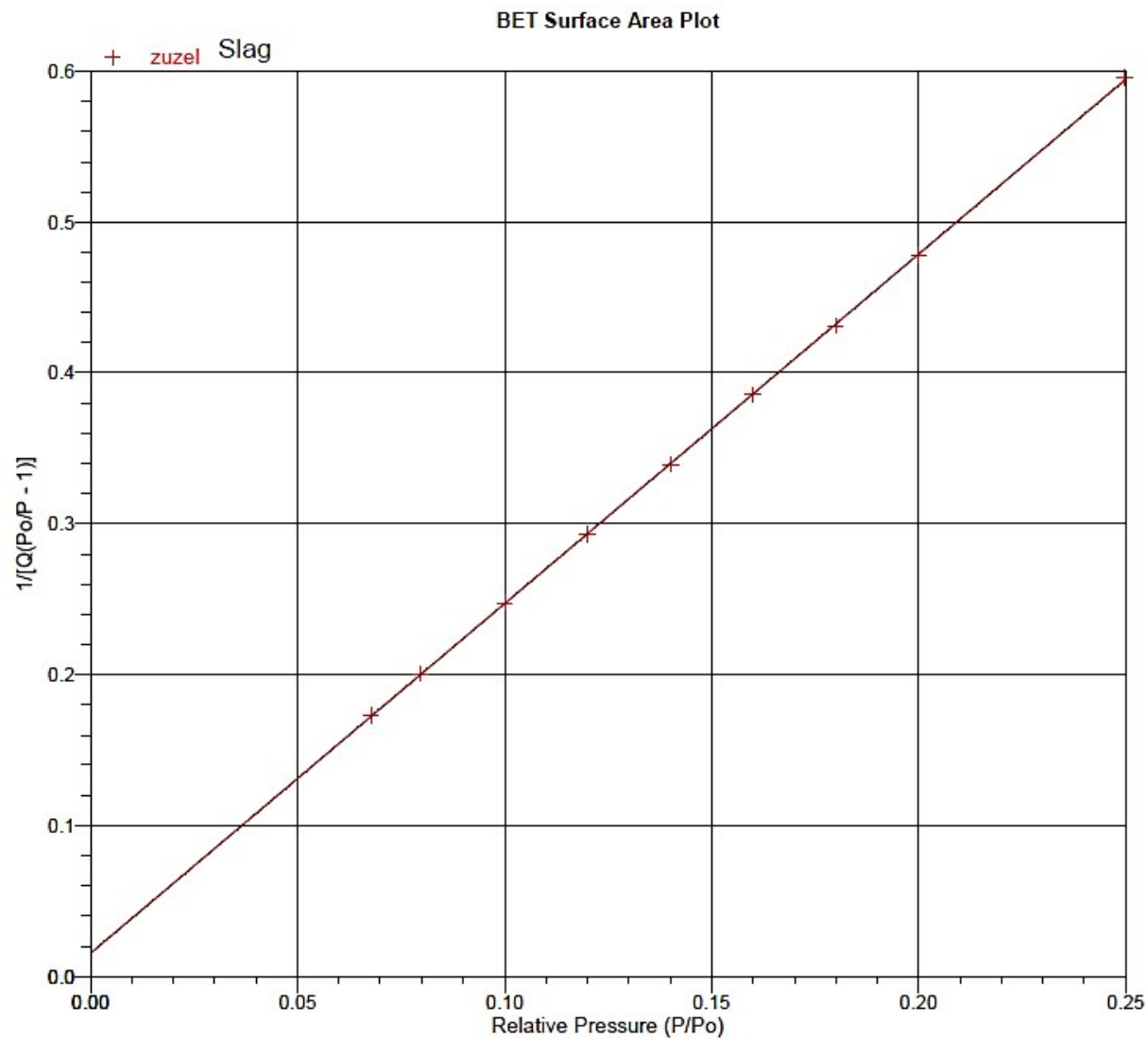


Fig. SM12. The linear BET isotherm of CFBC slag

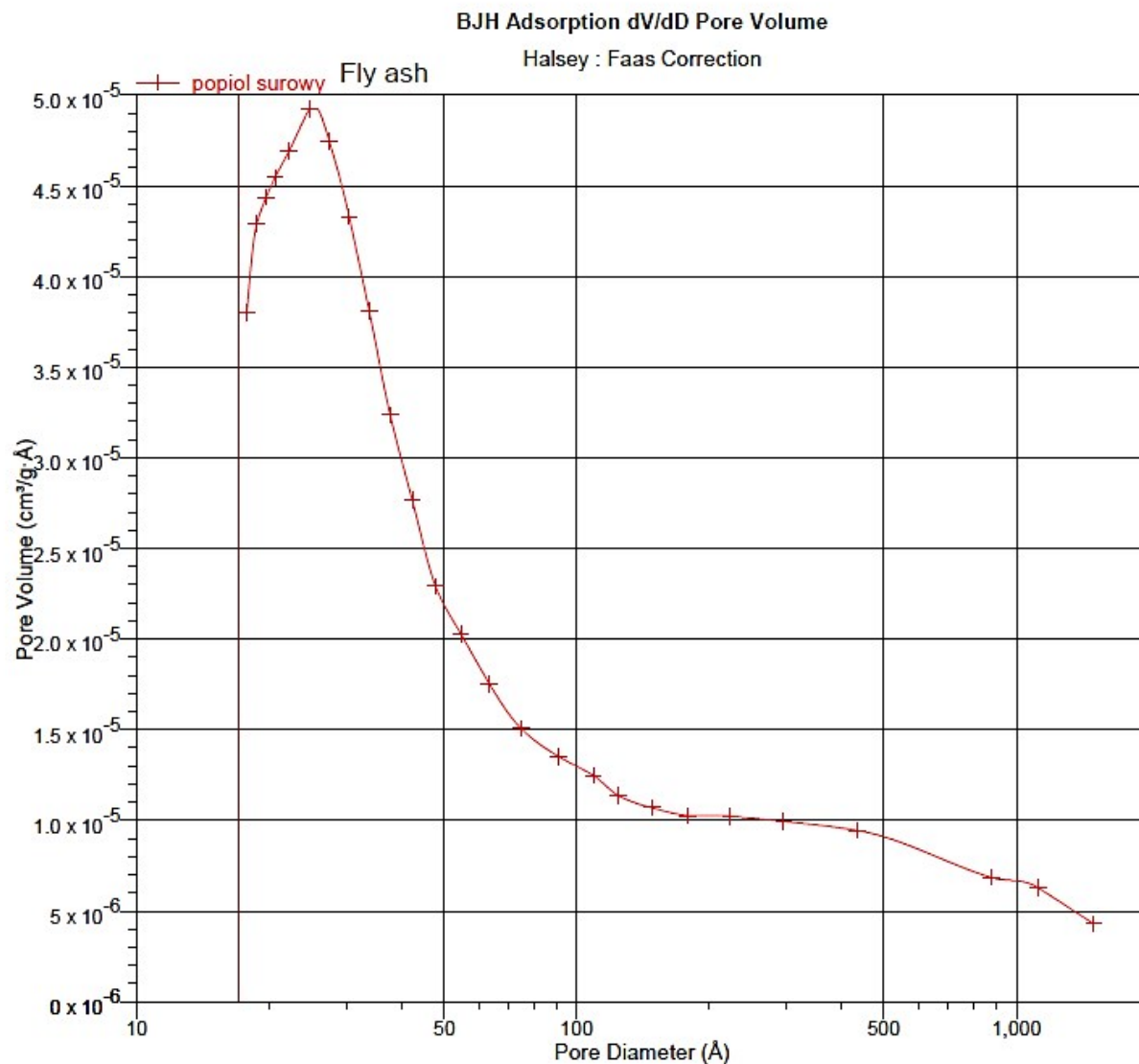


Fig. SM13. The BJH adsorption isotherm of CFBC fly ash

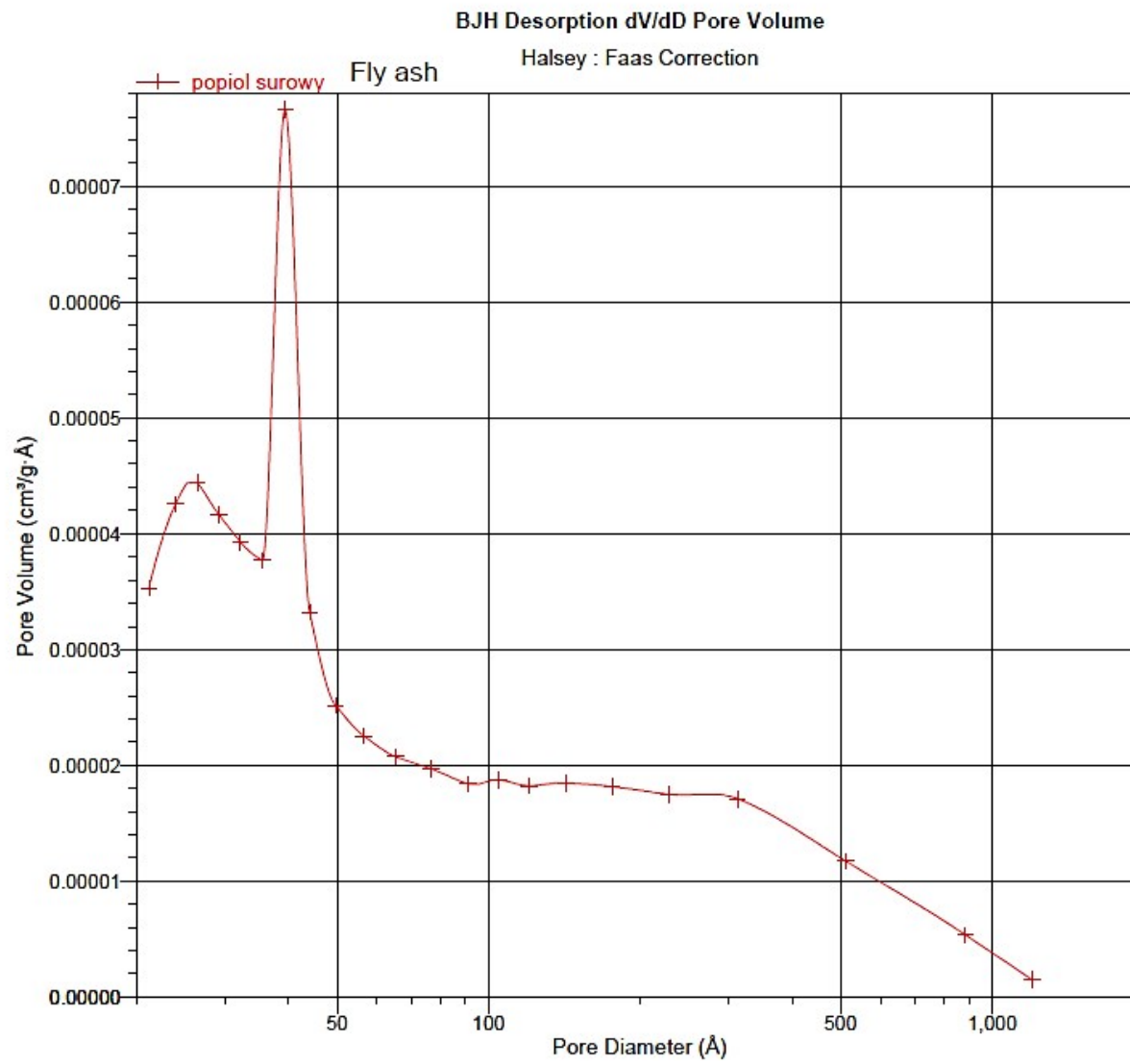


Fig. SM14. The BJH desorption isotherm of CFBC fly ash

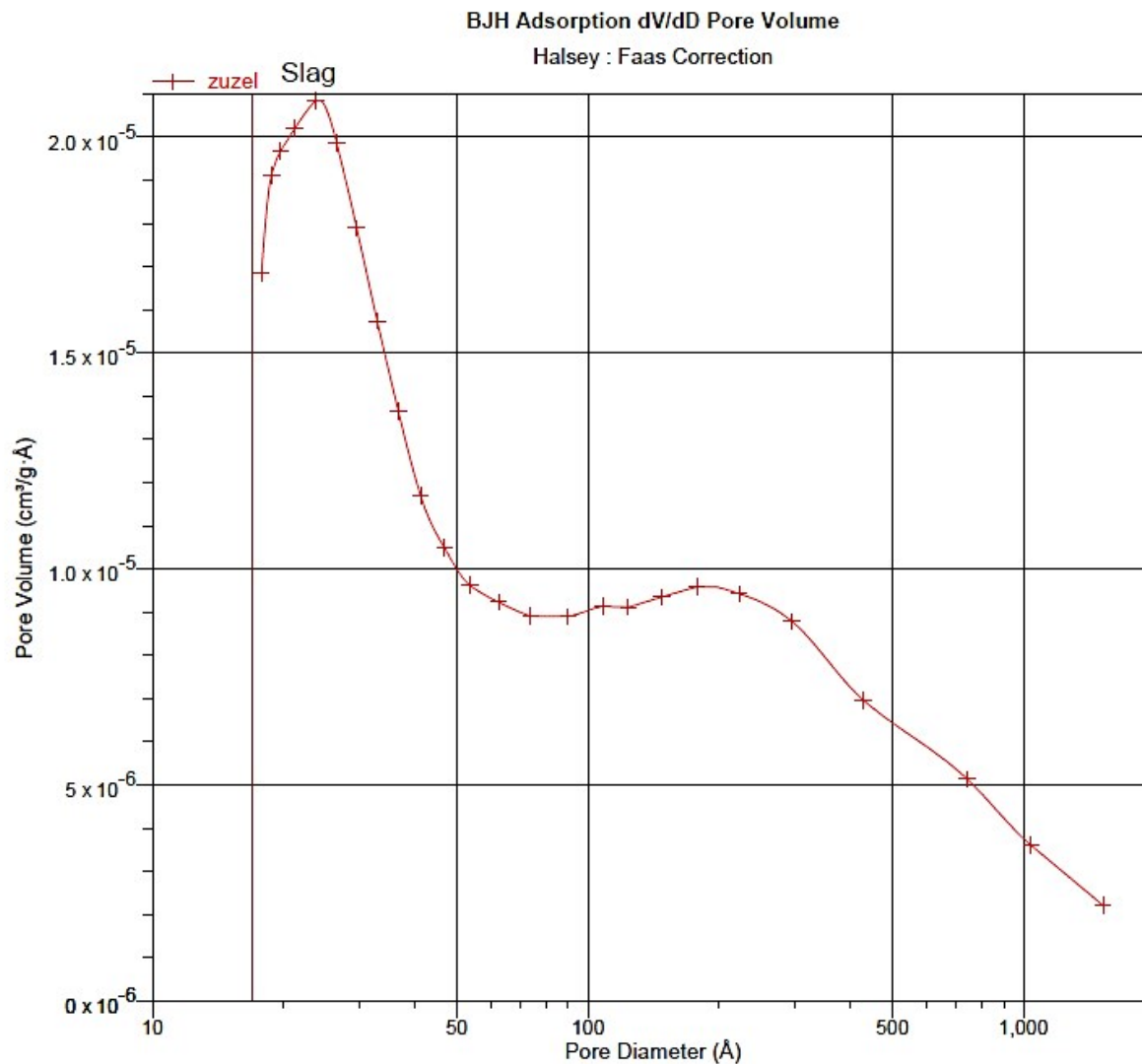


Fig. SM15. The BJH adsorption isotherm of CFBC slag

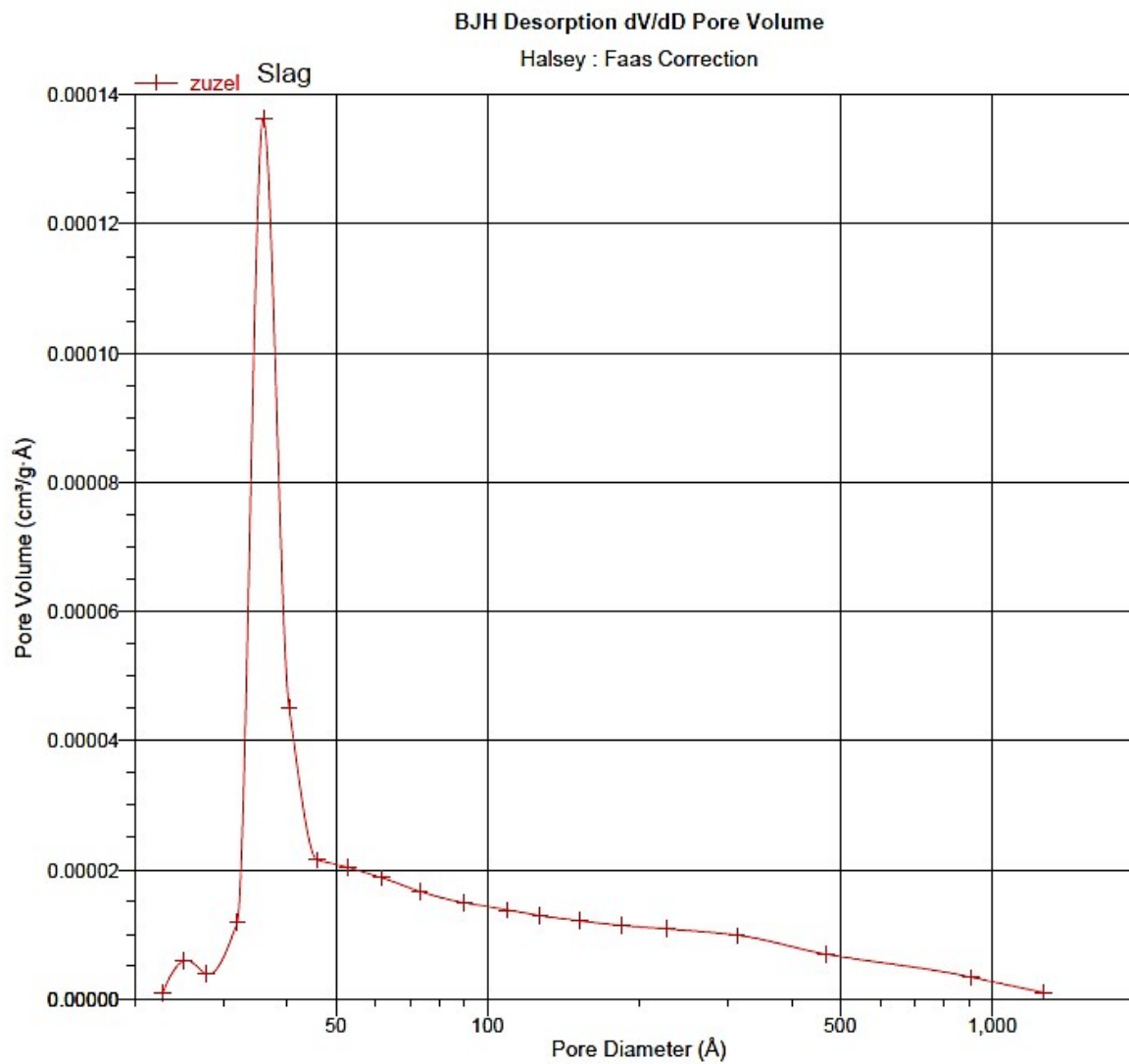


Fig. SM16. The BJH desorption isotherm of CFBC slag